Combining Ground Penetrating Radar Scans of Differing Frequencies Through Signal Processing

Roger Tilley, Hamid Sadjadpour
Department of Electrical Engineering
University of California, Santa Cruz
Santa Cruz, CA. 95064
Email: rtvax@soe.ucsc.edu, Email: hamid@soe.ucsc.edu

Farid Dowla
Lawrence Livermore National Laboratory
Livermore, CA. 94550
Email: dowla1@llnl.gov

***Abstract*— Interference reduction is vital in delivering a clear usable signal, whether in the form of beamforming in a noisy environment of radar target responses, or effective communication in the presence of noise for mobile phone users, as examples. The methods used to render a cleaner signal can also be used to combine signals of various frequencies. In this paper we explore using an optimization problem solver, the Expectation-Maximization Algorithm, to define the weights to be used to combine multiple Ground Penetrating Radar frequency scans over the same target area. This approach exploits the Gaussian Mixture Model feature to combine the scans to produce a cleaner image at depth. Our method demonstrates a measured improvement toward producing a cleaner image.**

Keywords- Ground Penetrating Radar; Expectation-Maximization; Gaussian Mixture Model; Maximum Likelihood Parameter Estimation; Finite Difference Time Domain Method; GprMax .

I. INTRODUCTION

Ground Penetrating Radar (GPR) signal scans are used to illuminate terrain and buried objects at various depths. The frequency scan that generates the best illumination is different for each depth. In general, higher frequencies image objects and terrain closer to the surface in great detail while lower frequencies image objects deeper with less fidelity. Developing a way to combine high and low frequencies suggests that the resolution of the combined signal is increased to a lower depth. Determining how to weight each frequency signal to be combined for an optimal result, poses as an optimization problem to solve. In the literature a few methods have been proposed to solve this problem with varying success, all with a very similar approach. Methods by Dougherty[1], Booth[2] and Bancroft[3] all discussed ways to weight each signal used in the sum of each system of frequency traces.

Dougherty's effort to enhance the original GPR data involved direct wave removal, bandwidth enhancement, and cross-correlation analysis. Dougherty aligned each trace by the direct arrival pulse. Scaled each trace by the L2 norm of the direct arrival pulse then simply summed the frequency traces after removing the direct arrival pulse and equally weighting each trace.

Booth used weights derived from the maximum value of the frequency spectra of each trace. The value used to equalize the spectra provided the signal trace weighting prior to summation. Booth's weights were derived from a time-variant least squares analysis of the amplitude spectra of each frequency data set, referred to as optical spectral whitening.

Bancroft uses a ramped summation method where the higher frequency data is suppressed by the same amount the lower frequency data is enhanced over a portion of the two way transit time of a GPR trace, determined by Bancroft and referred to as amplitude envelope equalization.

Absent from these works are optimization problem solvers. We have chosen to investigate the use of an optimization problem solver referred to as the Expectation-Maximization (EM) Algorithm; using the data mixture feature of the EM Algorithm to develop optimal weights.

In this paper, we illustrate the EM Algorithm data mixture feature as it relates to GPR scans of different frequencies. The paper is organized as follows. In SECTION II, we describe the EM Algorithm data mixture process. In SECTION III, we present an EM algorithm test case. In SECTION IV, GPR scans over the same area are processed using EM Algorithm tools developed to combine the frequencies. SECTION V draws some conclusions from using this approach.

II. EXPECTATION-MAXIMIZATION ALGORITHM

The EM Algorithm, is often used to group like items contained in complex mixtures. Another use is to solve incomplete data problems by performing Maximum Likelihood (ML) Parameter estimation. An offshoot use for the EM algorithm is determining the membership weights of points in a cluster within a finite Gaussian mixture model [4][9]. This feature will be exploited to combine several frequency scans into a composite wave. The entire data set can be represented by other mathematical distributions but we used Gaussian because it is often used when the distribution for the real-valued random variables is unknown.

We can define a finite mixture model $f(x;\theta)$ of K components as mixtures of Gaussian functions:

$$f(\underline{x};\theta) = \sum_{k=1}^{K} \alpha_k p_k(\underline{x}|\,\theta_k) \qquad (1)$$

 ISBN: 978-1-61208-539-5

Where:

- $p_k(\underline{x}|\theta_k)$ are K mixture components with a distribution defined over $p(\underline{x}|\theta_k)$ with parameters $\theta_k = \{\underline{\mu}_k, C_k\}$ (mean, covariance)
- $p_k(\underline{x}|\theta_k) =$
$$\frac{1}{(2\pi)^{d/2}\,|C_k|^{1/2}}\, e^{-\frac{1}{2}\left(\underline{x}-\underline{\mu}_k\right)^T C_k^{-1}\left(\underline{x}-\underline{\mu}_k\right)} \quad (2)$$
- α_k are the mixture weights, where $\sum_{k=1}^{K}\alpha_k = 1$.
- $\{\underline{x}_i, \ldots\ldots\ldots, \underline{x}_n\}$ Data set for a mixture component in d dimensional space.

In each iteration of the EM Algorithm, there are 2 steps, the Expectation step (E-step) and the Maximization step (M-step). In this case the E-Step computes the conditional expectation of the group membership weights $(w_{ik}{}'s)$ for $\underline{x}_i{}'s$, adding unobservable data given θ_k. The M-Step computes new parameter values $\left(\alpha_k, \underline{\mu}_k, C_k\right)$ to maximize the finite mixture model using the membership weights. The E-Step and M-Step are repeated until stopping criteria is reached (convergence). Convergence is signaled by the log-likelihood of $f(\underline{x};\theta)$ not appearing to change substantially from one iteration to the next.

E-Step –

$$w_{ik} = \frac{p_k(\underline{x}_i|\theta_k)*\alpha_k}{\sum_{m=1}^{K} p_m(\underline{x}_i|\theta_m)*\alpha_m} \quad (3)$$

for $1 \le k \le K,\ 1 \le i \le N;$

with constraint $\sum_{k=1}^{K} w_{ik} = 1$

M-Step –

$$N_k = \sum_{i=1}^{N} w_{ik} \quad (4)$$

$$\alpha_k^{new} = \frac{N_k}{N}, \text{ for } 1 \le k \le K \quad (5)$$

$$\underline{\mu}_k^{new} = \left(\frac{1}{N_k}\right)\sum_{i=1}^{N} w_{ik} * \underline{x}_i \quad (6)$$

for $1 \le k \le K$

$$C_k^{new} =$$

$$\left(\frac{1}{N_k}\right)\sum_{i=1}^{N} w_{ik} * \left(\underline{x}_i - \underline{\mu}_k^{new}\right)\left(\underline{x}_i - \underline{\mu}_k^{new}\right)^T \quad (7)$$

Convergence (log likelihood of $f(\underline{x};\theta)$) –

$$\text{Log}\, l(\vartheta) =$$

$$\sum_{i=1}^{N} \log f(\underline{x}_i;\theta) =$$

$$\sum_{i=1}^{N}\left(\log \sum_{k=1}^{K} \alpha_k p_k(\underline{x}_i|\theta_k)\right) \quad (8)$$

III. EXPECTATION-MAXIMIZATION ALGORITHM TEST CASE

As a test case, we constructed a series of six sine waves (50, 150, 250, 350, 450 and 550 Hz) noted in Fig. 1, Fig. 2 and Fig. 3, which when weighted properly sum to the square wave of Fig. 4. As noted in Fig. 5, the result is not quite a square wave but well on the way. The apparent error can be attributed to the constraints associated with this implementation; specifically group membership weights, w_{ik} and/or mixture weights, α_k each constrained to sum to one. The weights normally sum to greater than 1 dependent on the number of signals added together. The constructed sine waves are harmonics of the square wave used

.

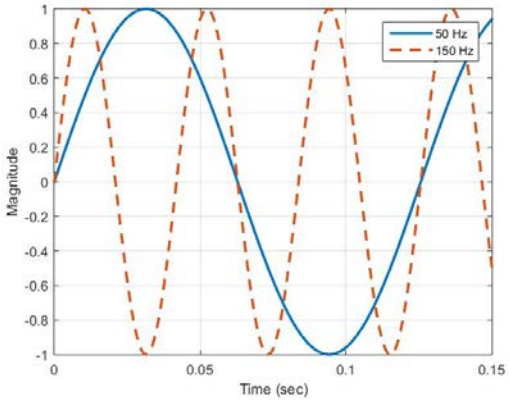

Fig. 1 – Sine wave frequencies 50-150 Hz

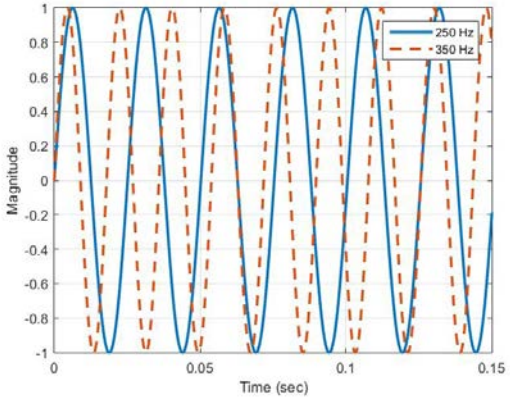

Fig. 2 –Sine wave frequencies 250, 350Hz

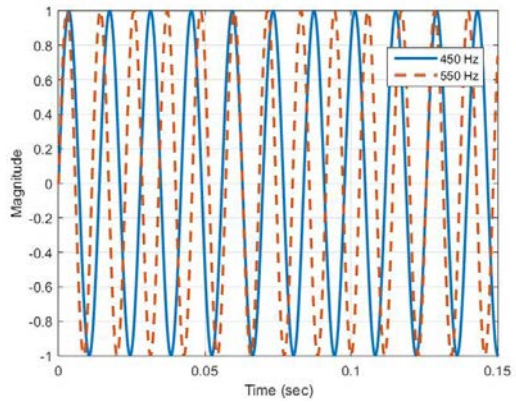

Fig. 3 – Sine wave frequencies, 450-550 Hz

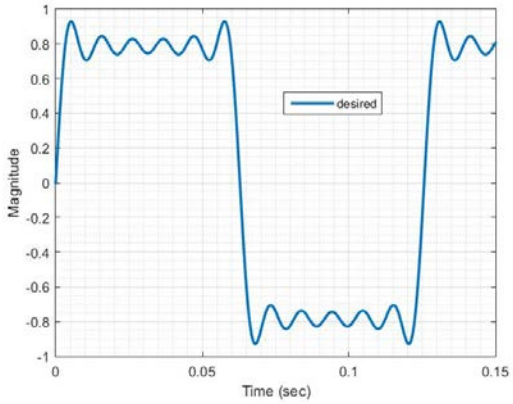

Fig. 4 – Square wave desired signal

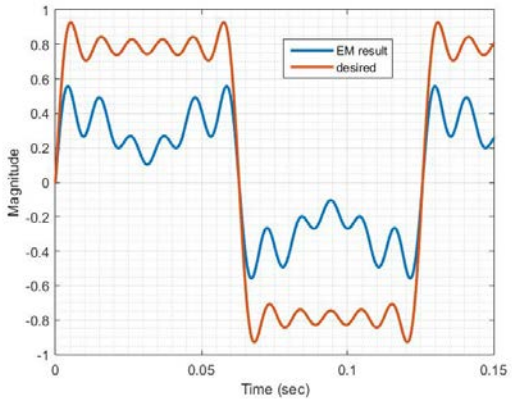

Fig. 5 – EM algorithm result with desired signal

IV. PROCESSING GPR SCANS AT VARIOUS FREQUENCIES

A fictional area was defined using a Finite Difference Time Domain (FDTD) [5][6][7] modeling software package. A Proprietary package in development similar in operation to the popular GprMax software program by A. Giannopoulos [8] was used to model a defined space. The space consisted of a Transmitter (Tx) and Receiver (Rx) suspended 5 meters above the ground in air with a target (perfect electrical conductor) buried 10 meters below ground in a moist-sand medium with a relative permittivity (ε_r) of 9.0 and an electrical conductivity of 0.001 mS/m. The transmitter and receiver were moved along the length of the defined space as shown in Fig. 6 for a total of 36 scans at 0.25 meters per step. The Tx starts at 0.5 meters ending at 9.5 meters, and the Rx starts at 0.75 meters ending at 9.75 meters well within the defined space of 10 meters in length by 25 meters in depth.

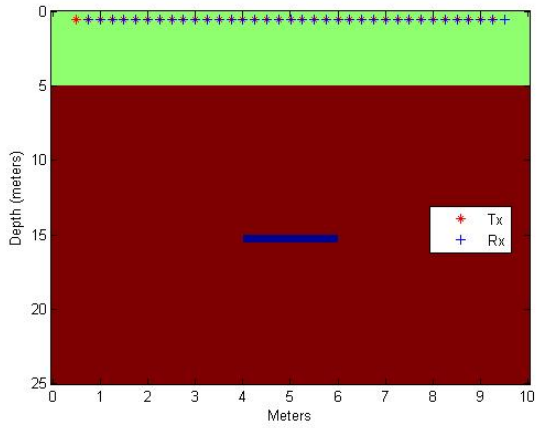

Fig. 6 Defined Space with buried target at 15 meters depth and Tx's & Rx's 5 meters above ground.

GPR scans over the same defined space were run at 20, 30, 50, 100, 500 and 900MHz. The resultant 2-D display for each frequency is shown in Figs. 7-14. Note that in each case the object is correctly identified at approximately 10 meters below ground, approximately 15 meters below Tx's and Rx's or approximately 240 ns from the direct arrival signal (black line on plot). In Fig. 12 and Fig. 14, a display of each trace is shown to better depict the target return signal. The direct arrival signal and ground bounce (radar return from the ground) are shown (see arrow 1 in Fig. 7). Arrow 2 in Fig. 7 denotes the target reflection at depth. In the 30MHz trace result (Fig. 8), the target is indicated by arrow 3. The remaining unlabeled arrows indicate the target reflection at depth for the indicated scan frequency. Of note, is the length of the line indicating the target in frequency scans 100MHz and below, representing limited if not non-existent edge detection. For this analysis the test area length is less than half the depth (25 meters depth by 10 meters length), more like a bore hole, contributing to the limited target edge detection. Arrow 4 (Fig. 14) exhibits better edge detection.

 ISBN: 978-1-61208-539-5

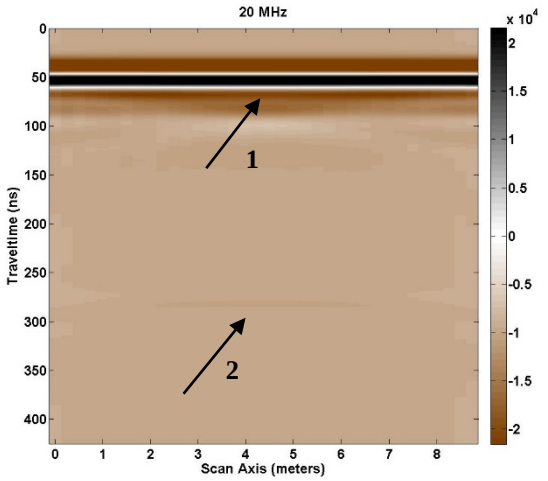

Fig. 7 2-D GPR scans 20MHz

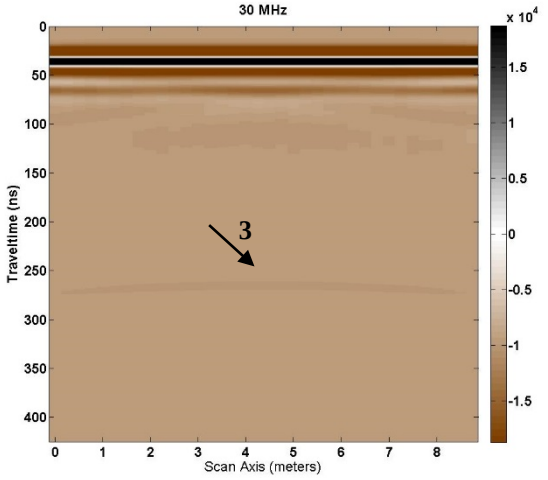

Fig. 8 2-D GPR scan 30 MHz

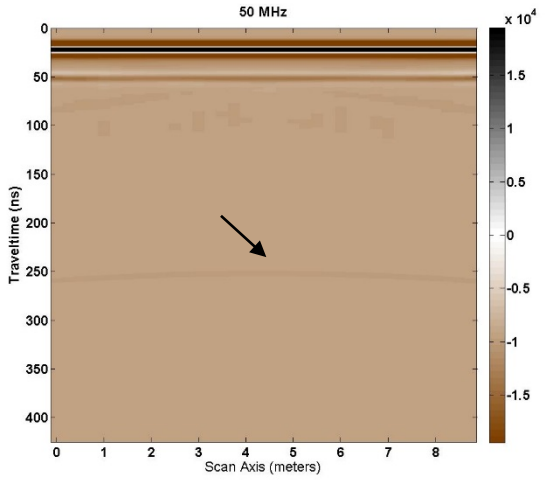

Fig. 9 2-D GPR scan 50 MHz

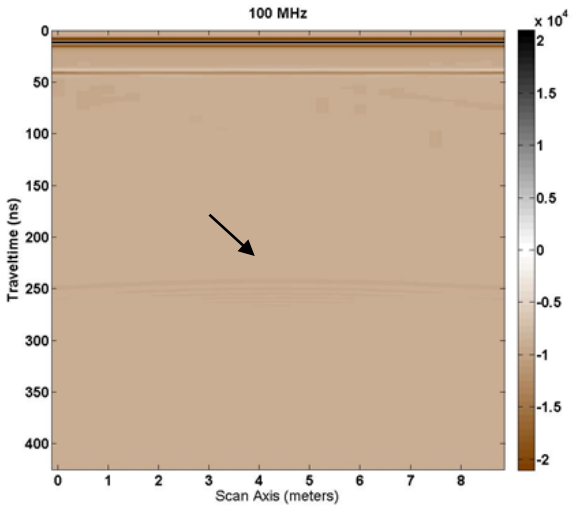

Fig. 10 2-D GPR scan 100MHz,)..

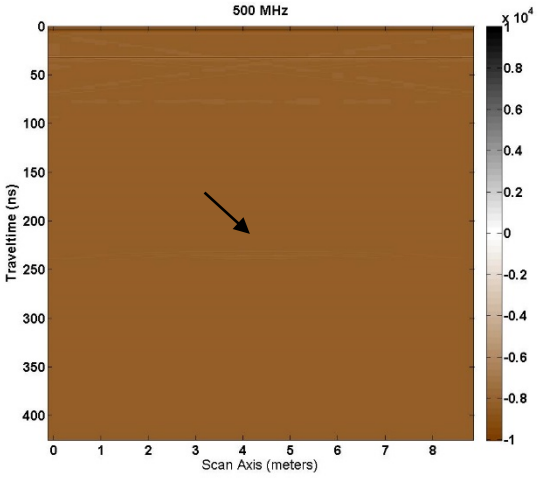

Fig. 11 GPR scan 500MHz

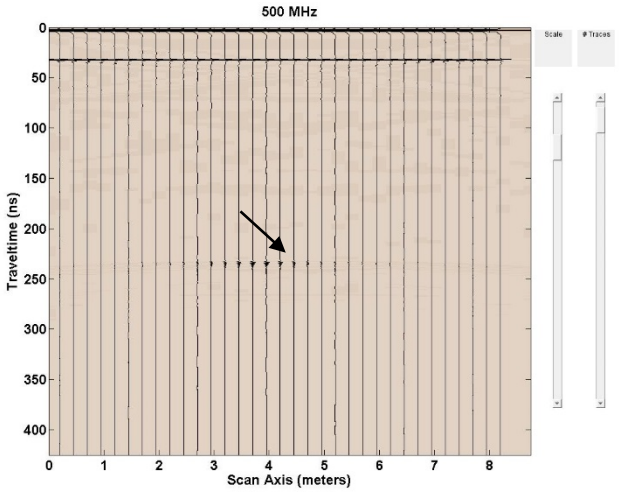

Fig. 12 GPR scan 500MHz (individual traces)

 ISBN: 978-1-61208-539-5

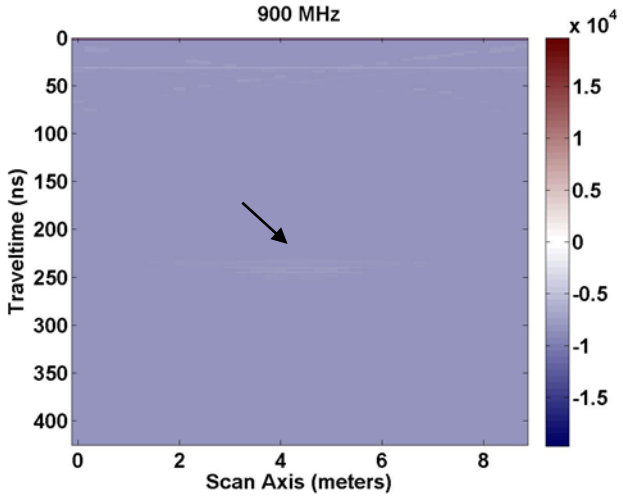

Fig. 13 GPR scan 900MHz (normal 2 D image display)

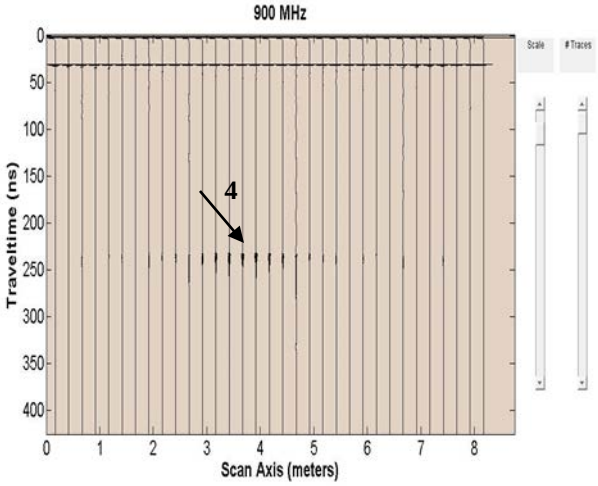

Fig.. 14 GPR scan 900MHz (individual traces)

In all of the GPR scan results, of note is that as the frequency is increased, the area where the target exists is more pronounced. The opposite occurs as the scan frequency is lowered.

Fig. 15 shows the result of adding each of the frequencies together having removed the direct arrival signal and scaling each signal max value to the same magnitude. A broad area of target reflection is shown from approximately 240 ns to 320 ns in depth (two-way travel time); a very rough indication of target depth.

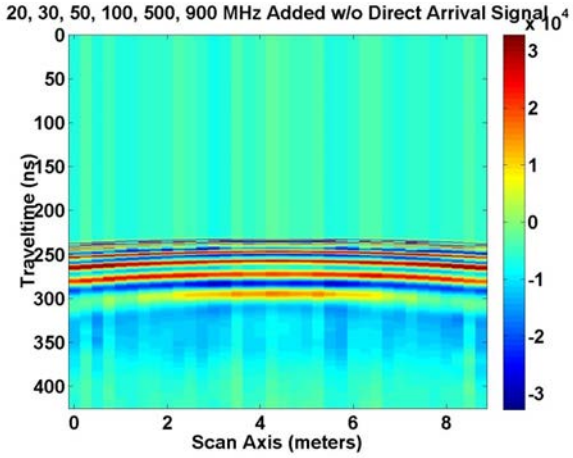

Fig. 15. Sum of frequency signals with direct arrival and ground bounce signals removed.

Fig. 16 and Fig. 17, show the same signals combined using the EM algorithm to determine the weight of each signal. Fig. 17 shows the EM processed individual signal traces. The area that is being scanned is more like a bore hole, twice as deep as it is wide. This accounts for the broad reverse "u-shaped" area that begins at target depth. The existence of lower frequencies in the sum broadens the output result.

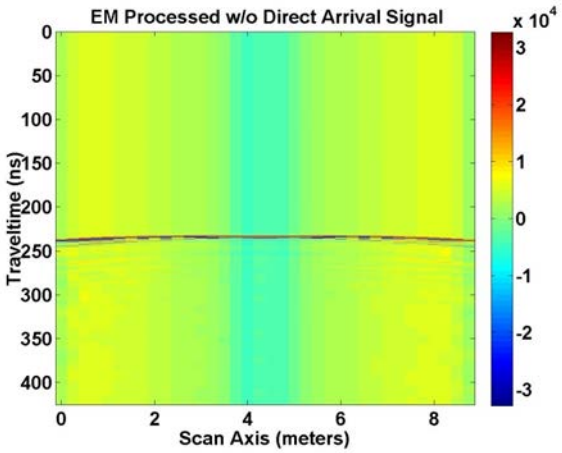

Fig. 16 EM sum of frequency signals with Direct Arrival and ground bounce signals removed.

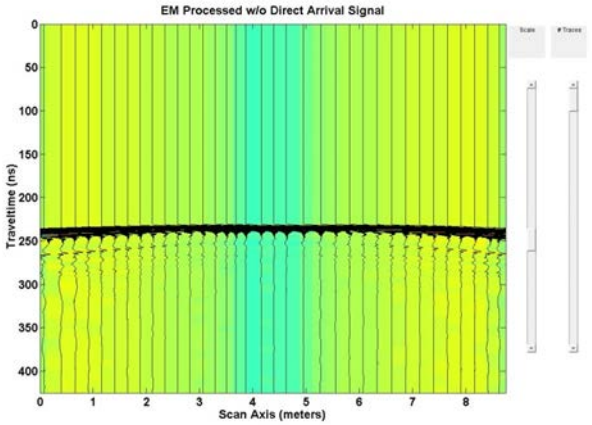

Fig. 17 EM processed signal traces with Direct Arrival and ground bounce signals removed.

As a test, a more complex structure was developed. This structure, Fig. 18, consists of an area 30 meters in length and 25 meters in depth with little or no space above ground, (0.15 meters), for the Tx and Rx used. The Tx and Rx are swept along the scan axis length starting at 0.5 meters (Tx) and ending at 24.85 meters with spacing between the Tx and Rx the same as before (0.25 meters). The number of GPR scans is 145. The electrical conductivity of the ground is the same as before but the relative permittivity (ε_r) is 3.0 for dry sand. Buried in the ground at 8 different levels (4.565m, 6.065m, 8.565m, 10.065m, 12.815m, 14.065m, 16.565m and 18.065m) are sheets of corrugated aluminum, modelled as perfect electrical conductors for ease of computation. Each sheet is approximately 2 meters in length and 0.1 meters thick. The GPR scanning frequencies are the same as before. The result for the EM method, shown in Fig. 19, identifies 8 targets at very close to the correct depth (approximately 50ns, 70ns, 100ns, 116ns, 148ns, 160ns, 190ns and 208ns for two-way travel time at a velocity in the medium of 0.1732 m/ns for the defined relative permittivity) with edges depicted reliably but with less fidelity as one descends in depth. Fig. 20 displays the individual GPR traces instead of the image response.

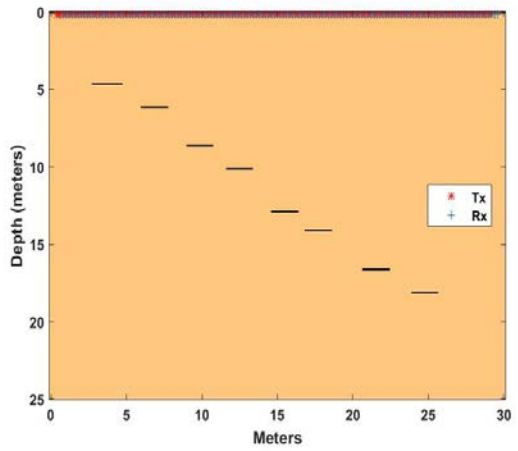

Fig. 18 EM algorithm Test Case, (8) 2m long plates, 0.1m thick

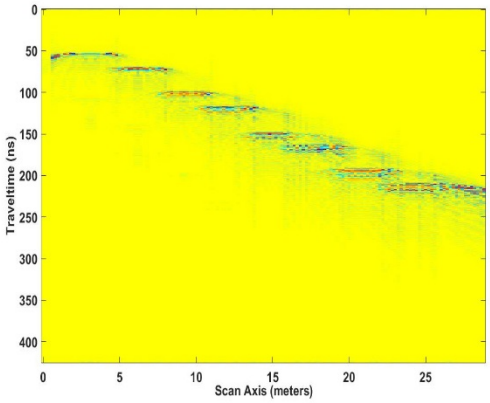

Fig. 19 GPR scan result for complex structure

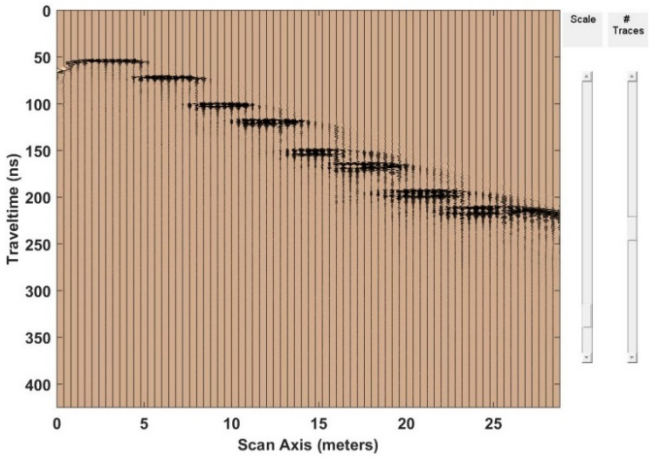

Fig. 20 EM processed signal traces for complex structure

V. CONCLUSIONS AND FUTURE WORK

We have shown that the Expectation and Maximization Gaussian Mixture Model approach to summing sine waves of a particular set of frequencies (harmonics of a square wave), works reasonably well. It is not, however, without problems associated with the magnitude of the calculated weights. As discussed earlier, the mixture weights are constrained to sum to 1; this is not what occurs in actuality. The result of summing sine waves was encouraging enough to continue this approach to GPR scans. Since actual equipment and a suitable target area were not available, computer codes were used to generate the scan area, the target, the type of material for the medium, and the resultant scans at several frequencies. The number of frequencies to use for this analysis was not defined at any time. We have illustrated that the computer code results is very similar to actual scans reported in an earlier paper [10]. We have further shown that just removing the direct arrival signal, the ground bounce, equalizing the magnitude of each frequency and adding the signals together is not sufficient. The result, though it points out the area of interest, the depth where the target appears is not well defined, Fig. 15. The depth indicator line is spread over 10s of nanoseconds. However,

 ISBN: 978-1-61208-539-5

the EM method confirms that a more definitive depth indication transpires than just adding the frequencies together, Fig. 16. A final test using a more complex structure demonstrates the viability of the EM algorithm method for GPR analysis, Figs. 19-20.

Our results illustrate that this approach is promising, however, further research is needed to prove its capability using more complicated simulated experiments and field experiments.

This work suggests more items to be explored like removing any DC shift in the data, any global background (mean trace) information in the data and any "wow" (signal interference, which manifests itself as low frequency signal added to the signal trace). Lining up each signal trace by the peak direct arrival pulse and reprocessing the data or looking at how the spectral bandwidth has been changed, are a few methods to investigate.

ACKNOWLEDGMENT

This work was performed under the auspices of the U.S. Department of Energy by Lawrence Livermore National Laboratory under Contract DE-AC52-07NA27344.

REFERENCES

[1] M. E. Dougherty, P. Michaels, J. R. Pelton, L. M. Liberty, "Enhancement of Ground Penetrating Radar Data Through Signal Processing", Symposium on the Application of Geophysics to Engineering and Environmental Problems 1994, pp. 1021-1028, Jan 1994, DOI 10.4133/1.2922053

[2] A. D. Booth, A. L. Endres, T. Murray, "Spectral Bandwidth Enhancement of GPR Profiling Data Using Multiple-Frequency Compositing", Journal of Applied Geophysics, vol 67, pp. 88-97, Jan 2009, DOI 10.1016/j.jappgeo.2008.09.015.

[3] S. W. Bancroft, "Optimizing the Imaging of Multiple Frequency GPR Datasets using composite Radargrams: An Example from Santa Rosa island, Florida", PhD dissertation, University of South Florida, 2010.

[4] Padhraic Smyth, "The EM Algorithm for Gaussian Mixtures, Probabilistic Learning: Theory and Algorithms, CS274A", University of California, Irvine, Department of Computer Science, Lecture Note 4.

[5] A. P. Annan, "Electromagnetic Principles of Ground Penetrating Radar," in Ground Penetrating Radar Theory and Applications, M. J. Harry, Ed., ed Amsterdam: Elsevier, pp. 1-40, 2009, ISBN: 978-0-444-53348-7.

[6] A. Tavlove, "Review of the formulation and Applications of the Finite-Difference Time-Domain Method for Numerical Modeling of Electromagnetic-Wave Interactions with Arbitrary Structures," Wave Motion, vol. 10, pp. 547-582, Dec 1988, DOI 10.1016/0165-2125(88)90012-1.

[7] N. Blindow, D. Eisenburger, B. Illich, H. Petzold, and T. Richter, "Ground Penetrating Radar," in Environmental Geology, Ed. Springer Berlin Heidelberg, pp. 283-235, 2008, DOI 10.1007/978-3-540-74671-3_10.

[8] A. Giannopoulos, "Modelling Ground Penetrating Radar by GprMax", Construction and Building Materials, vol. 19, pp. 755-762, Dec 2005, DOI 10.1016/j.conbuildmat.2005.06.007.

Article in Conference proceedings:

[9] J. J. Verbeek, N. Vlassis, and B. Kröse, "Efficient Greedy Learning of Gaussian Mixtures",The 13th Belgian-Dutch Conference on Artificial Intelligence (BNAIC'01),pp. 251-258, 2001, INRIA-00321510.

[10] R. Tilley, F. Dowla, F. Nekoogar, and H. Sadjadpour, "GPR Imaging for Deeply Buried Objects: A comparative Study based on FDTD models and Field Experiments, Selected Papers Presented at MODSIM World 2011 Conference and Expo; pp. 45-51, Mar. 2012; (NASA/CP-2012-217326); (SEE 20130008625) .

 ISBN: 978-1-61208-539-5